

IDENTIFICATION OF SEDIMENT-BASEMENT LAYER STRUCTURE IN WEST PAPUA PROVINCE INDONESIA BASED ON GRAVITY AND MAGNETIC INVERSION MODELING AS A STRESS INDICATOR OF EARTH CRUST

by Richard Lewerissa

Submission date: 12-Feb-2022 10:42PM (UTC+0900)

Submission ID: 1760722124

File name: Acta_Geophysica_final_submitted_revision_final.docx (13.79M)

Word count: 6558

Character count: 36325

1 IDENTIFICATION OF SEDIMENT-BASEMENT LAYER STRUCTURE IN WEST PAPUA
2 PROVINCE INDONESIA BASED ON GRAVITY AND MAGNETIC INVERSION MODELING
3 AS A STRESS INDICATOR OF EARTH CRUST

4 Richard Lewerissa^{1*} and Sismanto²

5 ¹Department of Physics, Faculty of Mathematics and Natural
6 Sciences, Papua University, Manokwari, Papua Barat 98314,
7 Indonesia

8 ²Department of Physics, Faculty of Mathematics and Natural
9 Sciences, Universitas Gadjah Mada, Yogyakarta 55281, Indonesia

10 *Corresponding Authors: r.lewerissa@unipa.ac.id
11

12 Abstract

13 Due to the convergence of the Australian, Pacific, and Eurasian tectonic plates, the province of West Papua
14 in eastern Indonesia is situated in a complicated tectonic setting. Many major strike-slip faults exist in this
15 interaction, including Koor, Sorong, Ransiki, and Yapen, where large and damaging earthquakes occur
16 frequently. According to regional geological conditions, rocks in the northern part of West Papua are the
17 contribution of the Pacific oceanic plate, which is composed of ophiolite and island arc volcanic, while
18 those in the southern part are dominated by quaternary and siliciclastic sedimentary rocks bounded from
19 west to east by the Sorong fault. Our research utilizes gravity and magnetic methods based on the
20 availability of regional satellite data to study the subsurface geological structure of sedimentary layers and
21 bedrock in the study area as an indication of stress on the earth's crust. The subsurface model was obtained
22 through three-dimensional (3-D) inversion modeling of gravity and magnetic anomalies data by first
23 performing separation and gradient analysis to improve the image of geological features. Gravity inversion
24 produces rock density contrasts ranging from -0.348 gr/cm³ to 0.451 gr/cm³, while magnetic inversion
25 produces rock susceptibility values between -0.363 SI to 0.223 SI, which are described in depth variations.
26 The gravity and magnetic inversions show the subduction of the Pacific Ocean plate in the northern part of
27 the bird's head of West Papua, massive intrusion of igneous rock, and the presence of low density and
28 susceptibility anomalies associated with the Bintuni Basin which is rich in oil and gas in eastern Indonesia.

29 The boundaries of the sedimentary and bedrock layers are estimated at a depth of between 15 - 20 km,
30 where the northern part of the bedrock layer is rock from the uplifted mantle, while in the southern part it
31 is mainly composed of the Silurian-Devonian Kemum formation.

32 **Keywords:** Gravity and magnetic; Inversion modeling; Sediment; Basement; West Papua.

33 34 1. Introduction

35 The western part of Papua Island is administratively one of the provinces in Indonesia. Tectonically,
36 this island is one of the most complex areas at the convergence boundary of the Australian and Pacific
37 plates and is at the forefront of understanding the overall tectonic process on Earth (Baldwin et al., 2012).
38 The Manokwari trough in the northern part of West Papua province is a subduction boundary of the
39 Caroline-Pacific oceanic crust beneath the Australian continental crust. This trough is assumed to be a
40 source of earthquake activity in the Bird's Head area of Papua, which is linked to significant strike-slip
41 faults including the Koor, Sorong, Ransiki, and Yapen (Daniarsyad & Suardi, 2017; Lewerissa et al., 2021).
42 There were 2807 earthquakes with magnitudes ranging from 3.5 to 7.7 between 1964 and 2021, most of
43 which were shallow earthquakes, while several large earthquakes caused significant damage in the area.
44 An earthquake hazard study is essential for determining the characteristics of future earthquake-prone sites
45 and preventing the negative impacts on civilization (Kalaneh & Agh-Atabai, 2016).

46 Previously, several seismic and geoscience studies in the West Papua region were conducted,
47 including determining the source mechanism of the 6.7 Mw earthquake at Ransiki in 2012 (Serhalawan &
48 Sianipar, 2017), fault studies to evaluate quaternary activity and indications of seismic hazard in West
49 Papua (Watkinson & Hall, 2017), and mapping of seismic hazard on Papua island in two regions, including
50 Indonesia and Papua New Guinea using probabilistic seismic hazard analysis (PSHA) (Makrup et al.,
51 2018). Furthermore, terrane gravity and tectonic measurements have been conducted in the New Guinea
52 region, indicating that the gravity method is an essential approach for terrane analysis but cannot be
53 employed for isolated structures (Milsom, 1991). According to the information, the research that has been
54 conducted is still restricted to studies on the ground surface and has not thoroughly investigated the
55 subsurface structure. Our research uses a potential field of geophysical method that aims to understand and
56 identify the structure of sediments and basements based on the availability of gravity and magnetic satellite
57 data.

58 The study was conducted to identify the stress level of the earth's crust in the West Papua region. In
59 2021, we have estimated the variation of Mc and b values from the USGS and ISC earthquake catalogs for
60 the period 1960 – 2021 and obtained the b values to be at the intermediate level for the West Papua region.
61 In general, the value of b is related to variations in stress and strain, fracture, and the rate of deformation.
62 This parameter can also indicate a high-stress level if the value of b is small (Lewerissa et al., 2021).

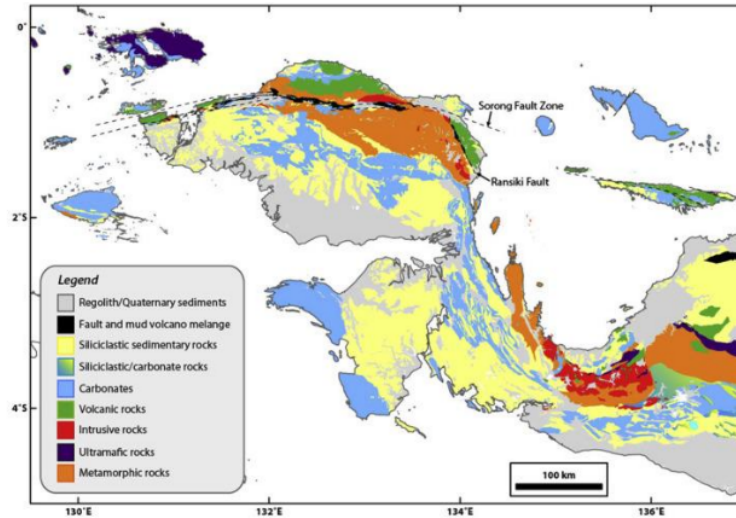
63 Geophysical data plays a significant part in the prediction and evaluation of seismic risks, which give
64 guidance about the geological formation of the crust. Gravity data aids in the development of models of the
65 crust and lithosphere at various scales, showing the density distribution of the upper crustal layers. On the
66 other hand, it provides a better understanding of the basin as a source of oil, gas, and water also detects
67 major tectonic features or structures (Saibi et al., 2021). Differences in crustal density are frequently related
68 to faults and tectonic features, which show a geological framework for seismic risk study. The density
69 defining of each layer that makes up the earth is critical for many investigations, including earthquake
70 studies, tectonic plate reconstruction, and modeling the petroleum system (Gómez-García et al., 2019; Tian
71 et al., 2020). It is known that in the study area there are two main basins producing the largest amounts of
72 oil and natural gas in eastern Indonesia, including the Salawati and Bintuni basins.

73 Satellites can detect fluctuations in the earth's magnetic field caused by various geological
74 characteristics of the lithosphere. Magnetic anomaly maps can provide critical things about tectonic
75 structures and the lithosphere in general. The gravity and magnetic techniques are relatively inexpensive,
76 non-invasive, and are non-destructive remote sensing methods. Furthermore, it involves information about
77 the density and variation of the magnetic susceptibility of rocks. This research uses the examination of the
78 earth's gravity gradient in the form of vertical, horizontal, and tilt angle derivatives to identify the borders
79 of geological formations such as major faults. The sedimentary and basement layer are derived from 3-D
80 inversion of regional gravity and magnetic anomalies data. These results are expected to be a support for
81 disaster mitigation or the search for new natural resources in West Papua region.

82 2. Geology and Tectonic Setting

83 New Guinea or Papua island is defined as having the shape of a bird from west to east, consisting a
84 bird's head, neck, body, and tail. The bird's head, tail, and part of its body are found in Papua and West
85 Papua, Indonesia, while the rest of the tail is found in Papua New Guinea (Gold et al., 2017b). Regionally,
86 the Papua island is influenced by two main activities that collide simultaneously until now. The Pacific

87 plate is moving southwest relative to the Australian plate at a speed of 11 cm/year, resulting in a complex
 88 tectonic structure (Handyarso & Padmawidjaja, 2017).



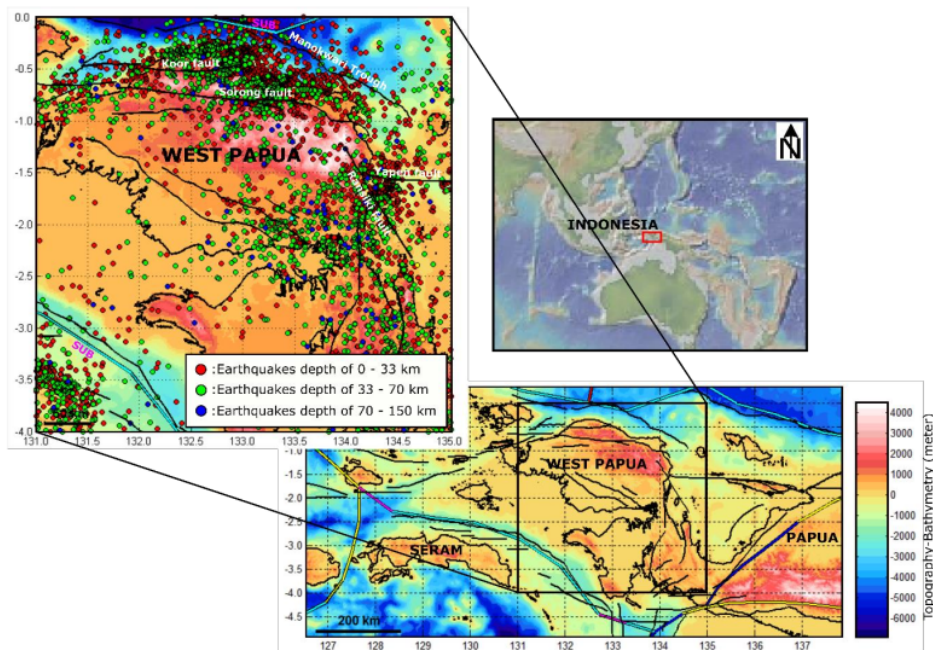
89
 90 Figure 1. Lithological map of western Papua, Indonesia depicting the main fault structure, dominated by
 91 volcanic, metamorphic, and sedimentary rocks (Gold et al., 2017b).

92 The neck is mostly made up of limestone and siliciclastic rocks that were shortened during the formation
 93 of the Lengguru fold belt. The rock is distorted as part of the mountain belt, which stretches from western
 94 Bird's Head to the eastern end of the island via the Lengguru fold and the central mountain range.
 95 In southern part of Papua island, rocks mainly from Australian continental plate, while the northern
 96 part consists of ophiolite and island volcanic arcs from the Pacific plate. These two domains are separated
 97 by a sedimentary wedge in the middle, as well as a variety of metamorphic and granitic rocks (Figure 1).
 98 This alignment is characterized by the presence of sutures formed during arc and continental collisions in
 99 the Oligocene and early Miocene. The Ransiki fault, located to the east of the bird's head, is thought to be
 100 due of a collision between an island arc and Australian continent, restricting into Cenderawasih Bay, east
 101 of Wandamen, and connecting with the Weyland overthrust in a Central Mountains (Gold et al., 2017a;
 102 Milsom, 1991; Milsom et al., 1992). Currently, the dominant arc rock forms the basement at the northern
 103 margin of Papua, the eastern bird's head, Cenderawasih Bay, and its islands. The Ransiki Fault is estimated
 104 to be a dextral shear zone with a NNW trend, connecting the Sorong Fault and the Yapen Fault, estimated

105 to be inactive (Charlton, 2010). The length of a typical segment of this fault ranges from 20 -50 km, while
 106 the maximum is around 100 km (Watkinson & Hall, 2017).

107 3. Methodology

108 Our study looks at the ²¹bird's head region in the Indonesian province of West Papua, which has unique
 109 and complex tectonic features. The coordinates of the research area are between 131° E – 135° E and 0° –
 110 4° S, which is an area that is prone to earthquakes ¹due to the collision of the Australian, Pacific, and Eurasian
 111 plates, as well as several other microplates.



112
 113 Figure 2. The research site in West Papua, Indonesia, is overlaid with topographic and bathymetric maps,
 114 as well as the main fault structures, which include the Sorong, Koor, Ransiki, and Yapen faults.

115 The historical seismic data from 1960 to 2021 obtained from the IRIS Data Management Center
 116 (<http://service.iris.edu/fdsnws/event/1>) shows that earthquakes mainly occurred in Koor, Sorong, Ransiki,
 117 and Yapen (Figure 2). This study integrates the interpretation and combination of regional gravity and
 118 magnetic potential field data based on satellite measurements to obtain the subsurface structure of West
 119 Papua.

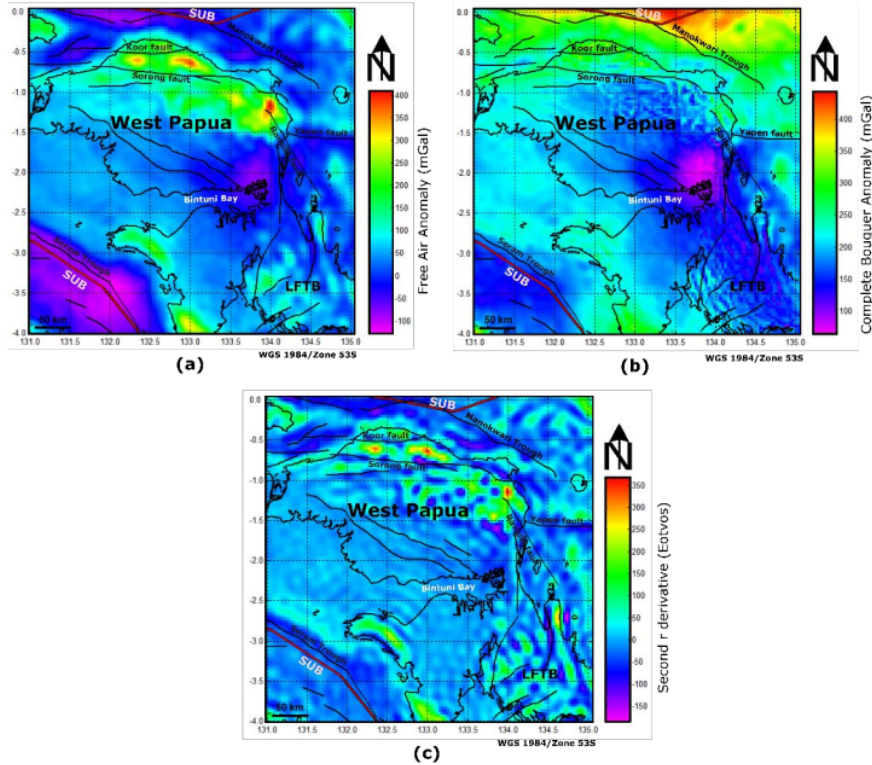
120 The gravity data is from the 2012 World Gravity Map (WGM), and it includes free air anomaly data
121 as well as the complete Bouguer anomaly (Balmino et al., 2012; Lewerissa et al., 2020). The second vertical
122 radial derivative data is from the XGM2019e model (Zingerle et al., 2020), and a magnetic data is from
123 NOAA's geomagnetic anomaly grid 2 version 3 (EMAG2-v3), with a spatial resolution of 2 arc minutes
124 (Lewerissa et al., 2020; Meyer et al., 2017). Moreover, the Global CRUST 1.0 model is used as a constraint
125 in 3D gravity and magnetic inversions (Laske et al., 2013).

126

127 3.1 Earth Gravity Data

128 The study utilizes the Earth's gravity method for mapping and delineating sedimentary and basement
129 structure boundaries in a West Papua using satellite gravity data from the 2012 WGM model. Global gravity
130 fields can be measured via satellite, which can reach areas where direct measurement is expensive and time-
131 consuming as in the sea (Gómez-García et al., 2019). WGM is a global gravity anomaly grid map calculated
132 with spherical geometry. It is derived from global earth gravity models like EGM2008 and DTU10, as well
133 as a 1' x 1' resolution field correction from the ETOPO1 model, which accounts for the majority of the
134 surface mass (Balmino et al., 2012). Free air and complete Bouguer anomalies of West Papua based on the
135 2012 WGM model are shown in Figure 3. Furthermore, XGM2019e is a model of the combined global
136 gravity field represented by spherical harmonics of degrees and orders of up to 5399 with a spatial resolution
137 of 2' arc minute (~4 km).

138 The model consists of the GOCO06s satellite model with wavelength ranges of up to degrees and order of
139 300, combined with a gravity grid model on the surface covering short wavelengths (Zingerle et al., 2020).
140 Surface data consists of gravity anomalies on land and ocean provided by the NGA with a resolution of 15',
141 plus topographically derived gravity information above the ground (EARTH2014). We use static model
142 calculations from an International Center for Global Earth Model (ICGEM) to obtain a second radial
143 derivative model (Ince et al., 2019) to define the boundaries of regional geological structures in the West
144 Papua region (Figure 3c). The complete Bouguer anomaly was then separated to obtain regional and
145 residual anomalies using an upward continuation technique at 4 km altitude from the surface.

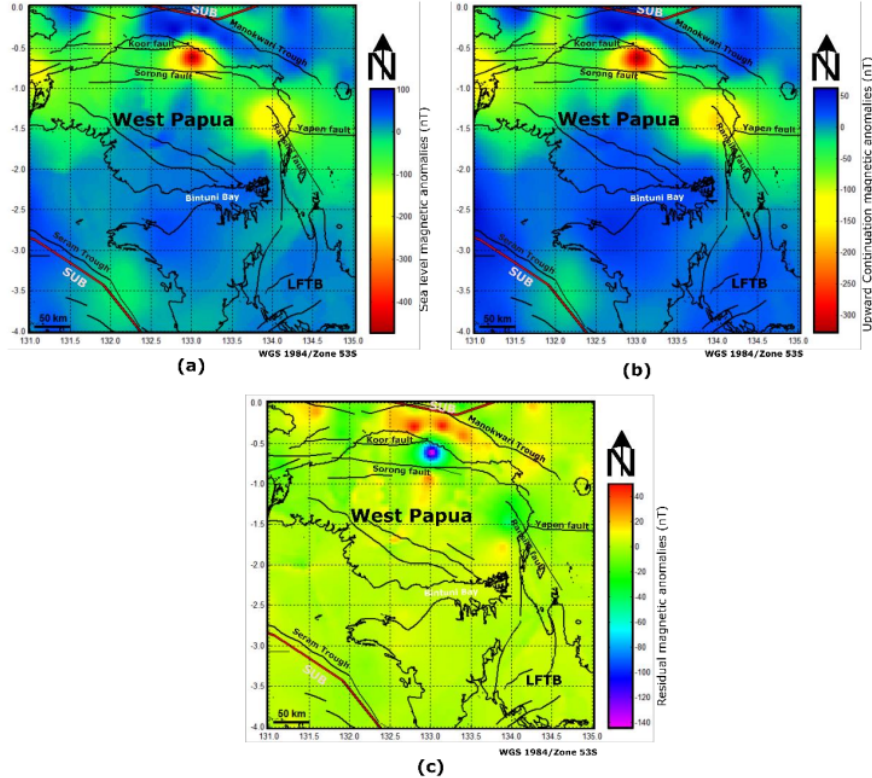


SUB: Subduction zone LFTB: Lengguru Fold Thrust Belt

Figure 3. The WGM 2012 and XGM2019 models of West Papua province. (a) Free air; (b) complete Bouguer; (c) Second r derivatives.

3.2 Earth Magnetic Data

The magnetic data utilized in this study is based on NOAA's EMAG2-v3 model, which is a collection of magnetic observations from satellites, ships, and aircraft. EMAG2-v3 is an updated model of the World Digital Magnetic Anomaly (WDMAM) map, which is gridded every 2 arc minutes and consists of two types of data, namely magnetic anomalies at sea level and upward continuation anomalies at 4 km from geoid (Meyer et al., 2017). We utilize Geoscience data services from Geosoft Seequent, which provide access to Geosoft Public DAP Server data (<https://public.dap.seequent.com/GDP/Search>), one of which is EMAG2-v3 data at sea level (Figure 4a) and upward continuation (Figure 4b) extracted for West Papua region.



158 **SUB:** Subduction zone **LFTB:** Lengguru Fold Thrust Belt
 159 Figure 4. EMAG2-v3 model in West Papua province (a) Sea level; (b) Upward continuation; (c) Residual
 160 anomaly.

161 The EMAG2-v3 model is very beneficial for obtaining a synoptic perspective of the magnetic field,
 162 and repeated observations of overlapping orbits may be used to reduce ionospheric extraneous magnetic
 163 fields caused by lithospheric abnormalities. These measurements are used to learn about the nature and
 164 history of other terrestrial entities (Hinze et al., 2013). Furthermore, the residual magnetic anomaly is
 165 determined by subtracting the sea level and the upward continuation anomalies (Figure 4c). The upward
 166 continuation data is then used for further analysis and inversion modeling without reduction to pole (RTP)
 167 because the study area is large enough that it will experience distortion in the application of RTP.

168 3.3 Earth Gravity Field Gradient

169 The gradient method of the Earth's gravity field, such as vertical, horizontal, and tilt angle derivatives,
170 is used in this study to enhance near-surface geological features that are not yet visible on a complete
171 Bouguer anomaly of West Papua. Gradient techniques using vertical and horizontal derivatives are also
172 used to describe the boundaries of geological structures and source objects buried in gravity fields. The
173 boundaries of geological structures and source objects buried in gravity fields are described using gradient
174 techniques in the form of vertical and horizontal derivatives (Eshaghzadeh et al., 2018). Vertical gradient
175 is commonly utilized highlight near-surface of geological structure and increase a component of
176 wavenumber spectrum, with a zero value corresponding to the geological structure's boundary (Ibraheem
177 et al., 2019). The vertical gradient equation is written as:

$$VG = \frac{\partial g}{\partial z} \quad (1)$$

178 Furthermore, a density contrast boundaries of the gravity field data are determined using a horizontal
179 gradient. When compared to vertical gradient, this approach is more effective for depicting shallow or deep
180 sources (Abderbi et al., 2017). 2-D horizontal gradient equation is showed as:

$$HG(x, y) = \sqrt{\left(\frac{\partial g}{\partial x}\right)^2 + \left(\frac{\partial g}{\partial y}\right)^2} \quad (2)$$

181 g is complete Bouguer anomaly. Another analysis conducted on gravity field data in the West Papua region
182 is Tilt angle (TA). This technique is applied to enhance and sharpen the anomalous form of gravity or
183 magnetic. Tilt angle is a ratio of vertical and horizontal derivatives with a range of -90° to 90° . TA is denoted
184 by the following equations:

$$TA = \tan^{-1} \left(\frac{VG}{HG(x, y)} \right) \quad (3)$$

185 TA is positive above the source object, close to zero or zero characterizing the source boundary, and
186 negative values are generally outside the source (Eshaghzadeh et al., 2018; Ibraheem et al., 2019). Overall,
187 the gravity field gradient in the study area was analyzed using a 2-D fast Fourier transform by Fourpot
188 software (Shandini et al., 2018).

3.4 Inversion Modeling of Potential Field Data

In West Papua, subsurface structures in the form of density and susceptibility distributions of rocks were obtained through inversion modeling of gravity and magnetic data. Process of inversion was performed using Geosoft Oasis Montaj software version 9.10, which was based on several inversion equations (Li & Oldenburg, 1996). Inversion is a numerical computational process used to create models of physical variables from the subsurface, such as density contrast and susceptibility for gravity and magnetic data. This technique produces a quantitative solution that is easier when compared to forward modeling, which involves iterating through trial and error (Saibi et al., 2021). This research utilizes the VOXI earth modeling facility from Oasis Montaj for 3-D inversion modeling in West Papua (Figure 5a).

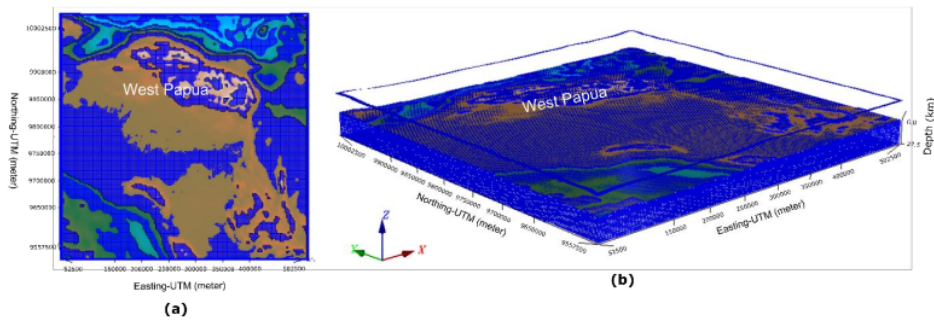


Figure 5. Reconstruction of a 3-D mesh model for the West Papua region (a) Digital Elevation Model; (b) 3-D grid model in the x, y, and z directions (blue lines indicate model boundaries).

The modeling begins with the reconstruction of initial model with a cell discretization of 180 x 178 x 17 for the x, y, and z directions, with a cell size of 2.5 km for the x and y, while for z up to 2.9 km (Figure 5b). Regional gravity anomalies and upward continuation magnetic anomalies up to 4 km are used as measurement data in the inversion modeling. The goal is to obtain the basement structure as well as the main basin in the area. At the midpoint of the West Papua region, the total magnetic field, inclination, and declination are 40433.16 nT, -20.14°, and 1.95°, respectively. This study also includes the CRUST 1.0 model as a constraint for gravity and magnetic data inversion modeling, with a resolution of 1° x 1°, CRUST 1.0 provides data on global surface topography, seabed bathymetry, seismic refraction, ice sheets, sediments, and the thickness of the earth's crust (Laske et al., 2013; Lewerissa et al., 2020). The Geoscience data service from Geosoft Seequent provided access to Geosoft Public DAP Server data

(<https://public.dap.sequent.com/GDP/Search>) in the form of subsurface density data (Figure 6a) and thickness of a crust (Figure 6b).

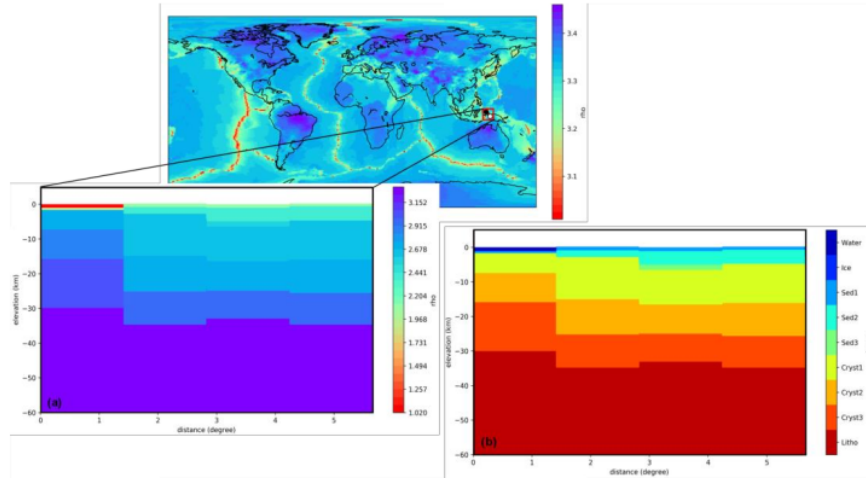


Figure 6. CRUST 1.0 cross-section in a West Papua, Indonesia, (a) Subsurface density distribution; (b) The earth's crust thickness.

4. Result and Discussion

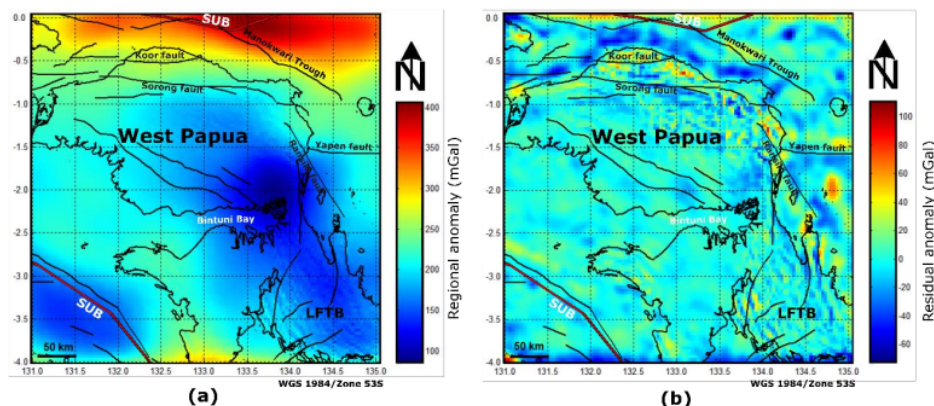
4.1. Regional and residual gravity anomalies in West Papua

The free-air gravity anomaly in the province of West Papua, Indonesia from the 2012 WGM model ranged from -127.64 mGal to 410.12 mGal (Figure 3a), while the complete Bouguer anomaly was positive between 63,830 mGal to 443.82 mGal (Figure 3b) covering land and sea areas. The free-air anomaly has a low value in the oceans to the north and northeast of the study area because they are in isostatic equilibrium, whereas it has a high value inland with higher topographic elevation, which is associated with mountain ranges. The complete Bouguer anomaly with high value is found in the northern and eastern parts of West Papua, and it is thought to be part of the mantle surface or Moho layer at shallow depths with high rock density. This high anomaly is also related to the northward subduction of the Pacific Ocean plate associated with the Manokwari Trough.

Furthermore, the value of the complete Bouguer anomaly decreased to the south and west, reaching a minimum value in the form of a circular shape at the neck of the bird, associated in the Bintuni basin with the main constituent composition of siliciclastic and quarter sedimentary rocks on the stratigraphy of the

230 Australian continental plate to the southeast on the Lengguru Fold Thrust Belt (LFTB). Low Bouguer
231 anomaly is generally correlated with positive elevation, whereas high anomaly is associated with negative
232 elevation. This correlation occurs ¹⁴ because the Bouguer anomaly is directly related to the density distribution
233 ⁵ in the crust and mantle (Gushurst & Mahatsente, 2020). Bird's head stratigraphy is broadly defined as intra-
234 ²⁹ Pacific island arc material to the north and east, followed by continental Australia material to the south and
235 west (Gold et al., 2017b). A low anomaly is also seen in the southwest part associated with the Seram trough
236 in Maluku province, thought to be a subduction zone of the Papuan bird's head microplate under the Banda
237 Sea (Putra & Husein, 2019).

238 The Sorong fault line from west to east is the ²⁶ boundary between the Pacific oceanic crust in the north
239 and the Australian continental crust in the south, according to the complete Bouguer anomaly map. A low
240 Bouguer anomaly has been studied in relation to the low seismicity parameter b, whereas the opposite is
241 thought to be related to the offshore free air anomaly. Temporal variations in the value of b are interpreted
242 as a result of seismicity migration by changes in spatial petrological, geophysical, and rheological
243 characteristics (El-Isa & Eaton, 2014). To emphasize the main regional geological structures in West Papua,
244 including Koor, Sorong, Ransiki, and Yapen faults, a second radial derivative map is also analyzed based
245 on the XGM2019e model. The value of the second radial derivative ranges from -184.93 Eotvos (mGal/km)
246 to 364.80 Eotvos (mGal/km), as shown in Figure 3c. On the second r derivative map, it is clear that the
247 main fault structure paths in the study area tend to be associated with zero values. In this route, earthquakes
248 predominantly occur in the province of West Papua. Subsequently, regional and residual gravity anomalies
249 were separated using an ² upward continuation technique at an altitude of 4 km based on a complete Bouguer
250 ² anomaly map. The height of the continuity is adjusted to the availability of EMAG2-V3 data upwards of 4
251 km.



(a) SUB: Subduction zone LFTB: Lengguru Fold Thrust Belt

Figure 7. Gravity anomalies separation in the West Papua region, (a) Regional anomalies; (b) Residual anomalies.

The process is carried out to obtain regional anomalies and eliminate the influence of small structures from the gravity data in form of residual anomalies. Regional gravity anomalies are used as input data for gravity inversion modeling to obtain a basement model in the study area. The positive regional gravity anomaly ranged from 85.90 mGal to 406.08 mGal (Figure 7a), while the residual gravity anomaly ranged from -72.45 mGal to 110.40 mGal (Figure 7b). The high regional anomaly is located in the north of West Papua and decreases towards the south with a circular pattern at the neck of the associated bird in the Bintuni basin. Residual anomalies are more complex than regional anomalies, with a predominance of moderate to low values. The high residual anomaly is distributed in several places, especially on the Koor fault line in the north, the Sorong fault and the Ransiki fault in the southeast, it is thought to be related to the volcanic rock lithology which has a high density (Figure 2). Regional gravity anomalies generally describe large and deep geological structures, while residual anomalies are associated with small and shallow structures.

4.2. Gravity Gradient in West Papua

The Earth's gravity gradient analysis aims to increase structural boundaries or geological contacts in the West Papua region not yet visible on the complete Bouguer anomaly map. The vertical gradient was negative to positive and ranged from -20.97 mGal/km to 19.61 mGal/km (Figure 8a). High gradient values were found in the north of the research area, while low values were distributed in several locations, such as the heads and necks of southern birds. In general, major fault structures and geological contact points in the

study area are related with a zero value of the vertical gradient. Positive values for the horizontal gradient
 range from 0.039 mGal/km to 16.56 mGal/km.

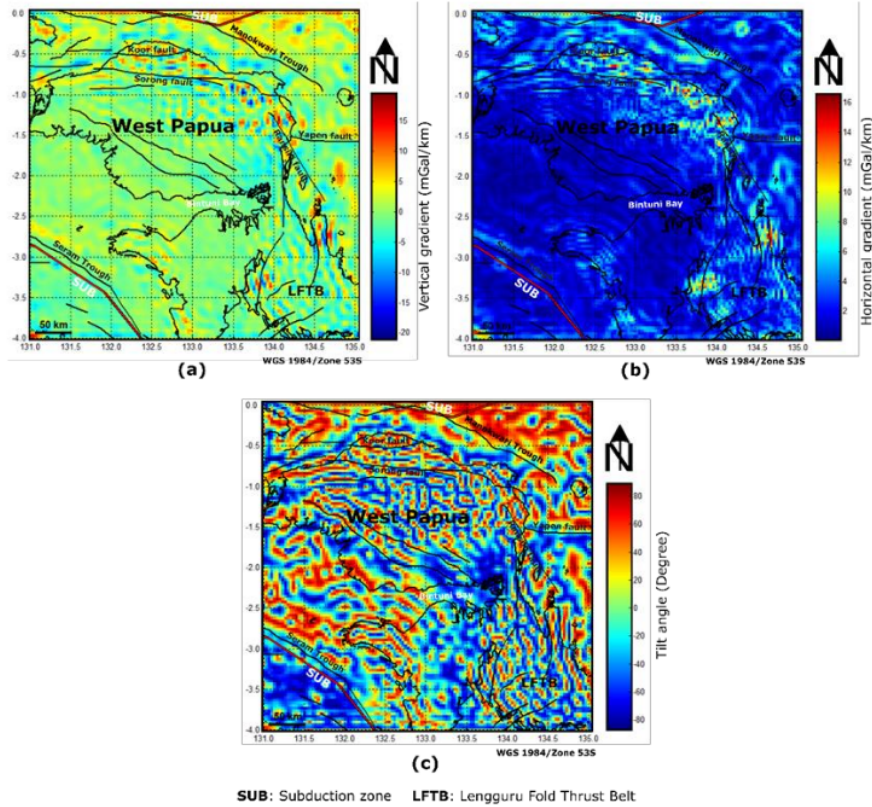


Figure 8. Earth's gravity gradient in West Papua; (a) Vertical gradient, (b) Horizontal gradient, (c) Tilt angle.

The maximum amplitude values on the horizontal gradient map of the West Papua region indicate geological contact boundaries, faults, and main geological structures (Figure 8b). Furthermore, tilt angle analysis is used to compute the arctan value of the ratio of vertical and horizontal gravity anomaly derivatives for the complete Bouguer anomaly data set. Tilt angle analysis has the advantage of not requiring physical parameters such as density, magnetic susceptibility, inclination, structural index, and so on in its calculations when compared to other methods. The tilt angle contour can be used to calculate the depth of the source (Akin et al., 2011). Tilt angle analysis of the complete Bouguer anomaly in West Papua produces more complicated values and patterns than vertical and horizontal gradients. The tilt angle value

286 ranges from -87.03° to 88.50° , with positive values predominating in the study area's north, east, and west
287 (Figure 8c), and negative values generally associated with the contact boundaries of geological structures
288 and major faults in West Papua. The vertical limit of the source of the anomaly or geological structure is
289 represented by the zero value of the tilt angle.

290 4.3. Magnetic Anomaly in West Papua

291 The EMAG2-v3 model provides two types of magnetic anomaly data extracted for the West Papua
292 region, including sea level anomalies and an upward continuation of 4 km above sea level. The sea-level
293 magnetic outliers ranged from -472.75 nT to 101.94 nT (Figure 4a), while the upward continuation
294 magnetic anomalies at 4 km altitude ranged from -328.178 nT to 62.001 nT (Figure 4b). Overall, the
295 patterns of magnetic anomalies for both models are relatively the same, with high anomalies predominant
296 in the north associated with the Manokwari Trough subduction zone, and then high anomalies are also
297 found at the bird's neck in the south. Low magnetic anomalies dominate Bird's Head from west to east,
298 mainly on the Koor, Sorong, Ransiki, and Yapen strike-slip fault lines.

299 The high-to-low magnetic anomalies in both models suggest west-to-east subduction from the north
300 of Bird's Head, a contribution from the Pacific Plate. Low negative anomalies with circular shapes were
301 found on the main Sorong and Koor fault lines and at two locations on the Ransiki fault line in the South
302 Manokwari District, possibly due to igneous intrusions in the study area. Such low magnetic anomalies are
303 generally associated with low rock susceptibility values in which volcanic rocks lose their magnetism due
304 to high temperature and high pressure. To further emphasize the magnetic anomalies that can describe
305 smaller geological structures, residual anomalies were also calculated based on the difference between sea-
306 level outliers and results that carried over up to 4 km. Residual outliers ranged from -144.57 nT to 49.86
307 nT (Figure 4c). The high residual anomaly further emphasizes the geological contact boundary indicating
308 subduction in the northern part of the Papuan bird's head, associated with the Manokwari trough of Pacific
309 oceanic crustal rocks.

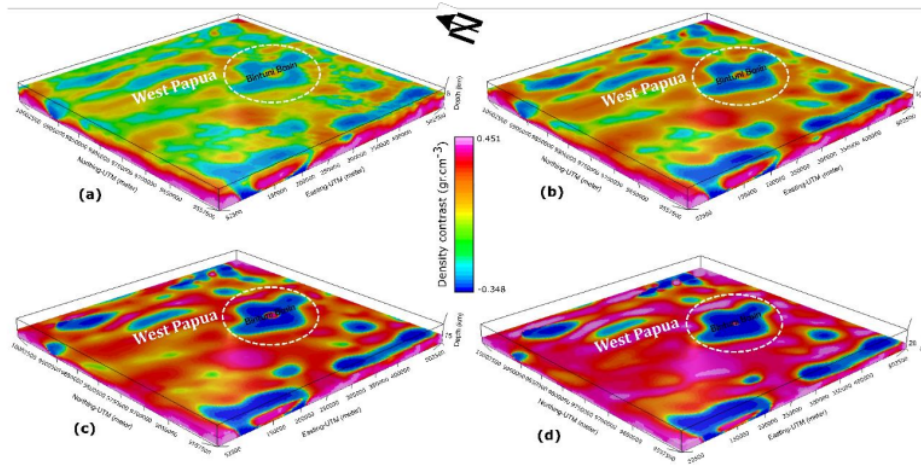
310 4.4. Gravity and Magnetic Anomalies Inversion

311 Figure 9 depicts the results of a three-dimensional inversion of regional gravity anomaly data in the
312 province of West Papua. The rock density contrast values obtained range from -0.348 gr/cm³ to 0.451
313 gr/cm³. The results of the gravitational inversion are represented as layers at various depths, including 5

314 km (Figure 9a), 10 km (Figure 9b), 15 km (Figure 9c), and 20 km (Figure 9d) (Figure 9d). At a depth of 5
 315 km, rock density contrast is generally moderate to low, with low-density contrast found in several locations
 316 in the north, bird's neck, southwest, and southeast. This low value is thought to be a result of the study area's
 317 tectonic activity. The geological structures of the main faults, such as the Sorong, Koor, Ransiki, and Yapen
 318 faults, are generally found at the boundary of low and high-density contrasts, particularly in the northern
 319 part of the bird's head from west to east.

320 In particular, the low-density contrast in a neck is associated with the Bintuni Basin which is the
 321 largest oil and gas producing basin in eastern Indonesia. The basement rocks of the Bintuni Basin are
 322 composed of the Kemum formation of Silur-Devon (Paleozoic) age, consisting of claystone, graywackes,
 323 and coarse clastics. The Kemum Formation is estimated to have experienced the folding and intrusion of
 324 granite rocks (Handyarso & Padmawidjaja, 2017). At a depth of 10 km, high-density contrast is seen starting
 325 to dominate in the entire study area. At this depth, the Bintuni basin begins to be seen with low-to-minimum
 326 density contrast. At this depth, the contrast of low rock density is also still visible. The contrast of rock
 327 density at a depth of 15 km and 20 km generally has the same pattern, where high-density contrast reaches
 328 a maximum that dominates the entire area. When compared with the global crust model CRUST 1.0 for the
 329 West Papua region (Figure 6), this layer is estimated to be the boundary between the sedimentary layer and
 330 the upper crust, presumably as the basement layer in the study area.

331



332

Figure 9. Rock layering model at various depths based on regional gravitational anomaly inversion modeling in West Papua: (a) 5 km; (b) 10 km; (c) 15 km; (d) 20 km.

The EMAG2-v3 model also performed a 3-D inversion of regional magnetic data up to 4 km to support the results of the three-dimensional (3-D) inversion of gravity data. Magnetic susceptibility physical parameter values range from -0.363 SI to 0.223 SI. Depth changes, such as gravity data inversion, comprise the rock formation system. The pattern of rock susceptibility at 5 km depth (Fig. 10a) is more complex, with moderate to high susceptibility values in the north and south, and low susceptibility in the middle of the bird's neck in Papua. High rock susceptibility can be found primarily to the north and south at a depth of 10 km (Figure 10b). Rock susceptibility generally follows the same pattern at depths of 15 km (Figure 10c) and 20 km (Figure 10d), with high susceptibility in the north, west to east, and south in the middle. This high susceptibility is thought to be due to the Pacific oceanic crust's high rock density and richness in magnetic minerals. This layer is thought to be West Papua's basement layer. The low rock susceptibility of the oil and gas-rich Bintuni Basin corresponds to quarter and siliciclastic sedimentary deposits.

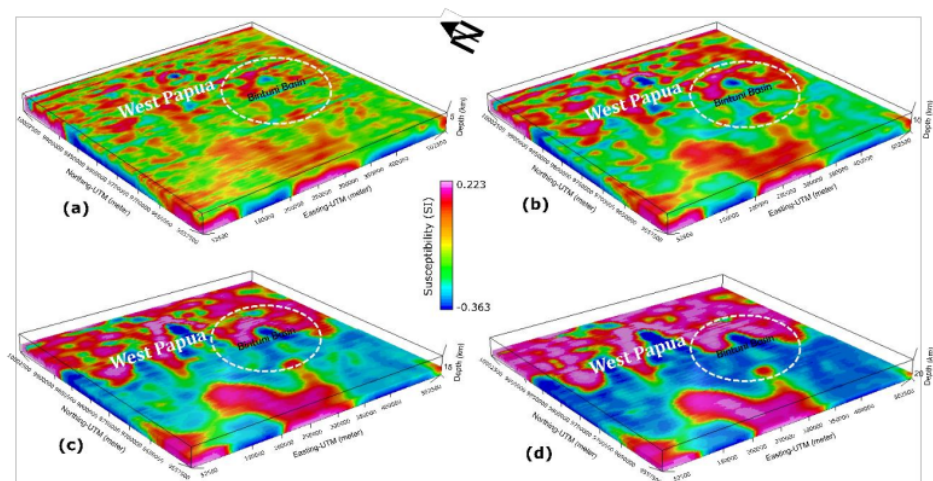


Figure 10. Rock layering model at various depths based on the upward continuation 4 km magnetic anomaly inversion modeling in West Papua: (a) 5 km; (b) 10 km; (c) 15 km; (d) 20 km.

The subsurface model is shown in the form of a north-south cross-section from the results of a three-dimensional (3-D) inversion to demonstrate the presence of tectonic activity in the province of West Papua (Figure 11). Figure 11a depicts a gravity inversion cross-section showing the subduction of the Pacific plate

with high rock density contrast under the Australian continental plate with lower density contrast from the north.

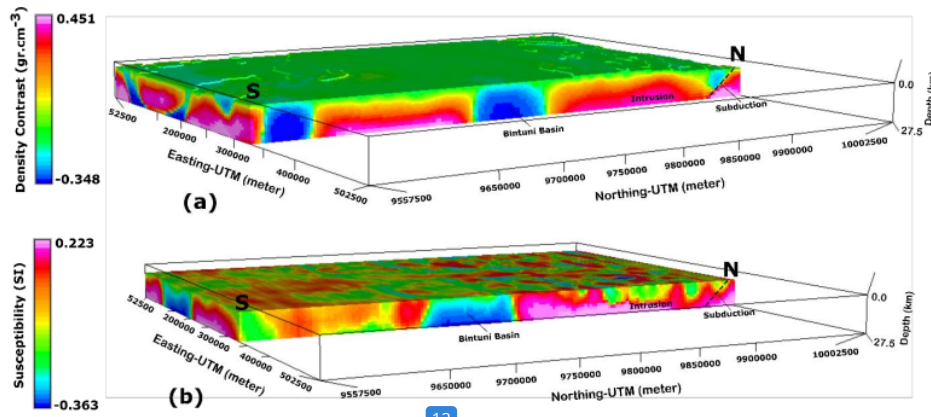


Figure 11. North to south cross-sectional model showing the subduction pattern of the Pacific plate beneath the Australian plate in West Papua: (a) Gravity inversion results; (b) Magnetic inversion results.

There is also an intrusion pattern of granite rocks, particularly in the mountain clusters in the study area. Papua's bird's head experienced intense volcanic activity during the Triassic period, with evidence of granite found at several locations on the bird's head and the western and southwestern parts of Cenderawasih Bay. Anggi granite, Wariki granodiorite, and Warjori granite are all part of the Netoni intrusion complex (Gold et al., 2017b; Webb & White, 2016). The gravity inversion cross-sectional model also clearly shows the Bintuni basin with negative density contrast, presumably having good oil and gas potential in the area. Figure 11b is a cross section of the magnetic inversion which shows the same pattern as the earth's gravity inversion. The subduction of the Pacific plate is characterized by the presence of high rock susceptibility under the Australian continental plate with lower susceptibility. Granite intrusion patterns are also depicted through rocks with high susceptibility. A cross section model of the gravity and magnetic data shows the appropriate results regarding the subsurface geological structure in the province of West Papua.

368 **5. Conclusion**

369 Utilization and analysis of gravity and magnetic data based on satellite measurements from the 2012
370 WGM model and EMAG2-v3 provide significant results for understanding tectonic activity and
371 determining the subsurface structure model for sediment-basement layers in West Papua. High gravity and
372 magnetic anomalies ² in the northern part of the study area indicate subduction of the high density and
373 magnetic mineral-rich Pacific plate under the Australian plate in the southern part which is associated with
374 low gravitational and magnetic anomalies. ³ Gravity gradient analysis in the form of vertical, horizontal, and
375 ²⁰ tilt angle derivatives provides results that confirm the boundaries of major geological structures such as the
376 Sorong, Koor, Ransiki, and Yapen faults, which are the paths of earthquakes in West Papua.

377 The three-dimensional ³⁷ (3-D) inversion of gravity and magnetic data shows conformity of the
378 subsurface model that describes the subduction of the Pacific Ocean plate ¹ in the northern part of the bird's
379 head of West Papua, the presence of massive intrusion of igneous rock, as well as the presence of density
380 anomalies and low susceptibility indicating the presence of a basin. Bintuni is rich in oil and gas in eastern
381 Indonesia. The boundary of the sedimentary and basement layers is estimated at a depth of between 15 –
382 20 km with rock from the mantle in the north as the basement, and the Kemum formation consisting of
383 Silur-Devonian metamorphic siliciclastic rocks in the south.

17

Acknowledgments

The author would like to thank Gadjah Mada University for providing the opportunity to participate in the 2021 post-doctoral program with grant number: 6144/UN1.P.III/DIT-LIT/PT/2021. The authors also thank the International Bureau of Gravity Survey (BGI) for the WGM 2012 gravity data and the National Oceanic and Atmospheric Administration (NOAA) for the EMAG2-V3 data, which are freely accessible for research. Thanks also to Seequent for the opportunity to model the inversion of gravity and magnetic data in West Papua using the Oasis Montaj 9.10 software.

Author Contributions: R.L. has developed the research concepts and designs, as well as written the manuscript. S.S. writes and assesses research findings in the form of a published manuscript.

Data availability

The datasets used in this study are available upon reasonable request from the corresponding author.

Competing interests

The authors state that they do not have any competing interests.

REFERENCES

- Abderbi, J., Khattach, D., & Kenafi, J. (2017). *Multiscale analysis of the geophysical lineaments of the High Plateaus (Eastern Morocco): Structural implications*. 10.
- Akin, U., Şerifoğlu, B. İ., & Duru, M. (2011). THE USE OF TILT ANGLE IN GRAVITY AND MAGNETIC METHODS. *Bulletin of the Mineral Research and Exploration*, 143(143), 1–12.
- Baldwin, S. L., Fitzgerald, P. G., & Webb, L. E. (2012). Tectonics of the New Guinea Region. *Annual Review of Earth and Planetary Sciences*, 40(1), 495–520. <https://doi.org/10.1146/annurev-earth-040809-152540>
- Balmino, G., Vales, N., Bonvalot, S., & Briais, A. (2012). Spherical harmonic modelling to ultra-high degree of Bouguer and isostatic anomalies. *Journal of Geodesy*, 86(7), 499–520. <https://doi.org/10.1007/s00190-011-0533-4>

- 410 Charlton, T. R. (2010). *The Pliocene-Recent Anticlockwise Rotation of the Bird's Head, the Opening of*
 411 *the Aru Trough – Cendrawasih Bay Sphenochasm, and the Closure of the Banda Double Arc.*
 412 http://archives.datapages.com/data/ipa_pdf/081/081001/pdfs/IPA10-G-008.htm
- 413 Daniarsyad, G., & Suardi, I. (2017). Stress triggering among $MW \geq 6.0$ significant earthquakes in
 414 Manokwari Trough. *AIP Conference Proceedings*, 1857(1), 020014.
 415 <https://doi.org/10.1063/1.4987056>
- 416 El-Isa, Z. H., & Eaton, D. W. (2014). Spatiotemporal variations in the b-value of earthquake magnitude–
 417 frequency distributions: Classification and causes. *Tectonophysics*, 615–616, 1–11.
 418 <https://doi.org/10.1016/j.tecto.2013.12.001>
- 419 Eshaghzadeh, A., Dehghanpour, A., & Kalantari, R. A. (2018). *Application of the tilt angle of the*
 420 *balanced total horizontal derivative filter for the interpretation of potential field data.* 59(2),
 421 161–178. <https://doi.org/10.4430/bgta0233>
- 422 Gold, D. P., Burgess, P. M., & BouDagher-Fadel, M. K. (2017). Carbonate drowning successions of the
 423 Bird's Head, Indonesia. *Facies*, 63(4), 25. <https://doi.org/10.1007/s10347-017-0506-z>
- 424 Gold, D. P., White, L. T., Gunawan, I., & BouDagher-Fadel, M. K. (2017). Relative sea-level change in
 425 western New Guinea recorded by regional biostratigraphic data. *Marine and Petroleum Geology*,
 426 86, 1133–1158. <https://doi.org/10.1016/j.marpetgeo.2017.07.016>
- 427 Gómez-García, Á. M., Meeßen, C., Scheck-Wenderoth, M., Monsalve, G., Bott, J., Bernhardt, A., &
 428 Bernal, G. (2019). 3-D Modeling of Vertical Gravity Gradients and the Delimitation of Tectonic
 429 Boundaries: The Caribbean Oceanic Domain as a Case Study. *Geochemistry, Geophysics,*
 430 *Geosystems*, 20(11), 5371–5393. <https://doi.org/10.1029/2019GC008340>
- 431 Gushurst, G., & Mahatsente, R. (2020). Lithospheric Structure of the Central Andes Forearc from Gravity
 432 Data Modeling: Implication for Plate Coupling. *Lithosphere*, 2020(1), 8843640.
 433 <https://doi.org/10.2113/2020/8843640>
- 434 Handyarso, A., & Padmawidjaja, T. (2017). Struktur Geologi Bawah Permukaan Cekungan Bintuni
 435 Berdasarkan Data Gaya Berat. *Jurnal Geologi dan Sumberdaya Mineral*, 18(2), 53–65.
 436 <https://doi.org/10.33332/jgsm.geologi.v18i2.125>

- 437 Hinze, W. J., von Frese, R. R. B., & Saad, A. H. (2013). *Gravity and Magnetic Exploration: Principles,*
438 *Practices, and Applications*. Cambridge University Press.
439 <https://doi.org/10.1017/CBO9780511843129>
- 440 Ibraheem, I. M., Haggag, M., & Tezkan, B. (2019). Edge Detectors as Structural Imaging Tools Using
441 Aeromagnetic Data: A Case Study of Sohag Area, Egypt. *Geosciences*, 9(5), 211.
442 <https://doi.org/10.3390/geosciences9050211>
- 443 Ince, E. S., Barthelmes, F., Reißland, S., Elger, K., Förste, C., Flechtner, F., & Schuh, H. (2019). *ICGEM*
444 *– 15 years of successful collection and distribution of global gravitational models, associated*
445 *services and future plans* [Preprint]. *Geosciences – Geodesy*. [https://doi.org/10.5194/essd-2019-](https://doi.org/10.5194/essd-2019-17)
446 17
- 447 Kalaneh, S., & Agh-Atabai, M. (2016). Spatial variation of earthquake hazard parameters in the Zagros
448 fold and thrust belt, SW Iran. *Natural Hazards*, 82(2), 933–946. [https://doi.org/10.1007/s11069-](https://doi.org/10.1007/s11069-016-2227-y)
449 016-2227-y
- 450 Laske, G., Masters, G., Ma, Z., & Pasyanos, M. (2013). Update on CRUST1.0—A 1-degree global model
451 of Earth's crust. *Abstract EGU2013-2658 Presented at 2013 Geophys. Res. Abstracts 15*, 15,
452 2658.
- 453 Lewerissa, R., Rumakey, R., Syakur, Y. A., & Laponi, L. (2021). Completeness magnitude (M_c) and b -
454 value characteristics as important parameters for future seismic hazard assessment in the West
455 Papua province Indonesia. *Arabian Journal of Geosciences*, 14(23), 2588.
456 <https://doi.org/10.1007/s12517-021-08885-4>
- 457 Lewerissa, R., Sismanto, S., Setiawan, A., & Pramumijoyo, S. (2020). *The igneous rock intrusion beneath*
458 *Ambon and Seram islands, eastern Indonesia, based on the integration of gravity and magnetic*
459 *inversion: Its implications for geothermal energy resources*. 29(4), 596–616.
460 <https://doi.org/10.3906/yer-1908-17>
- 461 Li, Y., & Oldenburg, D. W. (1996). 3-D inversion of magnetic data. *GEOPHYSICS*, 61(2), 394–408.
462 <https://doi.org/10.1190/1.1443968>
- 463 Makrup, L., Hariyanto, A., & Winarno, S. (2018). Seismic Hazard Map for Papua Island. *International*
464 *Review of Civil Engineering (IRECE)*, 9, 57. <https://doi.org/10.15866/irece.v9i2.14090>

465 Meyer, B., Chulliat, A., & Saltus, R. (2017). Derivation and Error Analysis of the Earth Magnetic
 466 Anomaly Grid at 2 arc min Resolution Version 3 (EMAG2v3). *Geochemistry, Geophysics,*
 467 *Geosystems*, 18(12), 4522–4537. <https://doi.org/10.1002/2017GC007280>

468 Milsom, J. (1991). Gravity measurements and terrane tectonics in the New Guinea region. *Journal of*
 469 *Southeast Asian Earth Sciences*, 6(3–4), 319–328. [https://doi.org/10.1016/0743-9547\(91\)90077-](https://doi.org/10.1016/0743-9547(91)90077-B)
 470 B

471 Milsom, J., Masson, D., Nichols, G., Sikumbang, N., Dwiyanto, B., Parson, L., & Kallagher, H. (1992).
 472 The Manokwari Trough and the western end of the New Guinea Trench. *Tectonics*, 11(1), 145–
 473 153. <https://doi.org/10.1029/91TC01257>

474 Putra, A., & Husein, S. (2019). *REGIONAL OVERVIEW OF OROGENIC BELTS IN INDONESIA:*
 475 *EMPHASIS ON THE OCCURRENCES OF THRUST WEDGE SYSTEMS*. 44, 19–41.

476 Saibi, H., Hag, D. B., Alamri, M. S. M., & Ali, H. A. (2021). Subsurface structure investigation of the
 477 United Arab Emirates using gravity data. *Open Geosciences*, 13(1), 262–271.
 478 <https://doi.org/10.1515/geo-2020-0233>

479 Serhalawan, Y. R., & Sianipar, D. S. J. (2017). *PEMODELAN MEKANISME SUMBER GEMPA BUMI*
 480 *RANSIKI 2012 BERKEKUATAN MW 6,7*. 6(1), 10.

481 Shandini, Y., Kouske, P. A., Nguiya, S., & Marcelin, M. P. (2018). Structural setting of the Koum
 482 sedimentary basin (north Cameroon) derived from EGM2008 gravity field interpretation.
 483 *Contributions to Geophysics and Geodesy*, 48(4), 281–298. [https://doi.org/10.2478/congeo-](https://doi.org/10.2478/congeo-2018-0013)
 484 2018-0013

485 Tian, T., Zhang, J., Jiang, W., & Tian, Y. (2020). Quantitative Study of Crustal Structure Spatial
 486 Variation Based on Gravity Anomalies in the Eastern Tibetan Plateau: Implication for
 487 Earthquake Susceptibility Assessment. *Earth and Space Science*, 7(3), e2019EA000943.
 488 <https://doi.org/10.1029/2019EA000943>

489 Watkinson, I. M., & Hall, R. (2017). Fault systems of the eastern Indonesian triple junction: Evaluation of
 490 Quaternary activity and implications for seismic hazards. *Geological Society, London, Special*
 491 *Publications*, 441(1), 71–120. <https://doi.org/10.1144/SP441.8>

492 Webb, M., & White, L. (2016). Age and nature of Triassic magmatism in the Netoni Intrusive Complex,
493 West Papua, Indonesia. *Journal of Asian Earth Sciences*, 132.
494 <https://doi.org/10.1016/j.jseaes.2016.09.019>
495 Zingerle, P., Pail, R., Gruber, T., & Oikonomidou, X. (2020). The combined global gravity field model
496 XGM2019e. *Journal of Geodesy*, 94. <https://doi.org/10.1007/s00190-020-01398-0>
497
498
499
500
501

IDENTIFICATION OF SEDIMENT-BASEMENT LAYER STRUCTURE IN WEST PAPUA PROVINCE INDONESIA BASED ON GRAVITY AND MAGNETIC INVERSION MODELING AS A STRESS INDICATOR OF EARTH CRUST

ORIGINALITY REPORT

17%

SIMILARITY INDEX

11%

INTERNET SOURCES

13%

PUBLICATIONS

1%

STUDENT PAPERS

PRIMARY SOURCES

1

link.springer.com

Internet Source

3%

2

journals.tubitak.gov.tr

Internet Source

3%

3

Richard Lewerissa, Nur Alzair, Laura Laponi. "Identification of Ransiki fault segment in South Manokwari Regency, West Papua Province, Indonesia based on analysis of a high-resolution of global gravity field: Implications on the Earthquake Source Parameters", IOP Conference Series: Earth and Environmental Science, 2021

Publication

2%

4

Richard Lewerissa, Rizal Rumakey, Yasir Abdan Syakur, Laura Laponi. "Completeness magnitude (M_c) and b-value characteristics as important parameters for future seismic hazard assessment in the West Papua

1%

province Indonesia", Arabian Journal of Geosciences, 2021

Publication

5	coek.info Internet Source	1 %
6	Earth-Planets-Space.springeropen.com Internet Source	<1 %
7	Richard Lewerissa, Sismanto Sismanto, Ari Setiawan, Subagyo Pramumijoyo, Laura Laponi. "Integration of gravity and magnetic inversion for geothermal system evaluation in Suli and Tulehu, Ambon, eastern Indonesia", Arabian Journal of Geosciences, 2020 Publication	<1 %
8	assets.researchsquare.com Internet Source	<1 %
9	www.science.gov Internet Source	<1 %
10	www.degruyter.com Internet Source	<1 %
11	Tian Tian, Jingfa Zhang, Wenliang Jiang, Yunfeng Tian. "Quantitative Study of Crustal Structure Spatial Variation Based on Gravity Anomalies in the Eastern Tibetan Plateau: Implication for Earthquake Susceptibility Assessment", Earth and Space Science, 2020 Publication	<1 %

12	earthjay.com Internet Source	<1 %
13	journal.lemigas.esdm.go.id Internet Source	<1 %
14	pubs.geoscienceworld.org Internet Source	<1 %
15	eartharxiv.org Internet Source	<1 %
16	"Geology of Southwest Gondwana", Springer Science and Business Media LLC, 2018 Publication	<1 %
17	dspace.unimap.edu.my Internet Source	<1 %
18	www.frontiersin.org Internet Source	<1 %
19	Min Li, Song Huang, Miao Dong, Ya Xu, Tianyao Hao, Xueshan Wu, Yufeng Deng. "Prediction of marine heat flow based on the random forest method and geological and geophysical features", Marine Geophysical Research, 2021 Publication	<1 %
20	pure.royalholloway.ac.uk Internet Source	<1 %
21	www.isc.hbs.edu Internet Source	

<1 %

22

Baishali Roy, Ron M. Clowes. "Seismic and potential - field imaging of the Guichon Creek batholith, British Columbia, Canada, to delineate structures hosting porphyry copper deposits", GEOPHYSICS, 2000

Publication

<1 %

23

Cesar Tapia, Vsevolod Yutsis, Nick Varley. "Crustal structure and magmatic system of Isla Socorro (Eastern Pacific Ocean), derived from the interpretation of geological-geophysical data", Acta Geophysica, 2021

Publication

<1 %

24

Da-Ren Fang, Gen-Hou Wang, Ken-ichiro Hisada, Guo-Li Yuan, Fang-Lin Han, Dian Li, Yu Tang, Qiu-Ming Pei, Liang-Liang Zhang. "Provenance of the Langjiexue Group to the south of the Yarlung-Tsangpo Suture Zone in southeastern Tibet: Insights on the evolution of the Neo-Tethys Ocean in the Late Triassic", International Geology Review, 2018

Publication

<1 %

25

Yihao Wu, Adili Abulaitijiang, Ole Baltazar Andersen, Xiufeng He, Zhicai Luo, Haihong Wang. "Refinement of Mean Dynamic Topography Over Island Areas Using Airborne Gravimetry and Satellite Altimetry Data in the

<1 %

Northwestern South China Sea", Journal of Geophysical Research: Solid Earth, 2021

Publication

26

journals.itb.ac.id

Internet Source

<1 %

27

Balaguru, A.. "Tertiary stratigraphy and basin evolution, southern Sabah (Malaysian Borneo)", Journal of Asian Earth Sciences, 200408

Publication

<1 %

28

Baldwin, Suzanne L., Paul G. Fitzgerald, and Laura E. Webb. "Tectonics of the New Guinea Region", Annual Review of Earth and Planetary Sciences, 2012.

Publication

<1 %

29

Benjamin M. Jost, Max Webb, Lloyd T. White. "The Mesozoic and Palaeozoic granitoids of north-western New Guinea", Lithos, 2018

Publication

<1 %

30

Constanza Rodriguez Piceda, Magdalena Scheck Wenderoth, Maria Laura Gomez Dacal, Judith Bott et al. "Lithospheric density structure of the southern Central Andes constrained by 3D data-integrative gravity modelling", International Journal of Earth Sciences, 2020

Publication

<1 %

31	Handbook of Geomathematics, 2015. Publication	<1 %
32	Milsom, J.. "Three trench endings in eastern Indonesia", Marine Geology, 19920229 Publication	<1 %
33	Richard A. Krahenbuhl. "Influence of self-demagnetization effect on data interpretation in strongly magnetic environments", SEG Technical Program Expanded Abstracts, 2007 Publication	<1 %
34	Robert Hall. "Cenozoic geological and plate tectonic evolution of SE Asia and the SW Pacific: computer-based reconstructions, model and animations", Journal of Asian Earth Sciences, 200204 Publication	<1 %
35	eprints.ucm.es Internet Source	<1 %
36	oceanrep.geomar.de Internet Source	<1 %
37	research.library.mun.ca Internet Source	<1 %
38	www.nevadasunrise.ca Internet Source	<1 %
39	Ángela María Gómez - García, Christian Meeßen, Magdalena Scheck - Wenderoth,	<1 %

Gaspar Monsalve et al. "3 - D Modeling of Vertical Gravity Gradients and the Delimitation of Tectonic Boundaries: The Caribbean Oceanic Domain as a Case Study", Geochemistry, Geophysics, Geosystems, 2019

Publication

40

Prasanta K. Patro. "Chapter 270 Magnetotellurics, Crustal Imaging", Springer Science and Business Media LLC, 2021

Publication

41

Richard Lewerissa, Sismanto Sismanto, Ari Setiawan, Subagyo Pramumijoyo. "The Study of Geological Structures in Suli and Tulehu Geothermal Regions (Ambon, Indonesia) Based on Gravity Gradient Tensor Data Simulation and Analytic Signal", Geosciences, 2017

Publication

42

D.P. Gold, L.T. White, I. Gunawan, M.K. BouDagher-Fadel. "Relative sea-level change in western New Guinea recorded by regional biostratigraphic data", Marine and Petroleum Geology, 2017

Publication

43

International Association of Geodesy Symposia, 2014.

Publication

<1 %

<1 %

<1 %

<1 %

44

Maurizio Fedi, Antonio Rapolla. "3-D inversion of gravity and magnetic data with depth resolution", GEOPHYSICS, 1999

Publication

<1 %

45

discovery.ucl.ac.uk

Internet Source

<1 %

Exclude quotes On

Exclude matches < 5 words

Exclude bibliography On